

Field-effect transistor made of individual V_2O_5 nanofibers

G. T. Kim,^{a),b)} J. Muster, and V. Krstic

Max-Planck-Institut für Festkörperforschung, Heisenbergstraße 1, D-70569 Stuttgart, Germany

J. G. Park and Y. W. Park

Department of Physics and Condensed Matter Research Institute, Seoul National University, Seoul 151-742, Korea

S. Roth and M. Burghard

Max-Planck-Institut für Festkörperforschung, Heisenbergstraße 1, D-70569 Stuttgart, Germany

(Received 17 September 1999; accepted for publication 4 February 2000)

A field-effect transistor (FET) with a channel length of ~ 100 nm was constructed from a small number of individual V_2O_5 fibers of the cross section $1.5\text{ nm}\times 10\text{ nm}$. At low temperature, the conductance increases as the gate voltage is changed from negative to positive values, characteristic of a FET with n -type enhancement mode. The carrier mobility, estimated from the low-field regime, is found to increase from $7.7\times 10^{-5}\text{ cm}^2/\text{V s}$ at $T=131\text{ K}$ to $9.6\times 10^{-3}\text{ cm}^2/\text{V s}$ at $T=192\text{ K}$ with an activation energy of $E_a=0.18\text{ eV}$. The nonohmic current/voltage dependence at high electric fields was analyzed in the frame of small polaron hopping conduction, yielding a nearest-neighbor hopping distance of $\sim 4\text{ nm}$. © 2000 American Institute of Physics. [S0003-6951(00)00714-2]

The fabrication of synthetic nanowires does not require high-resolution lithography, which makes them attractive as components of nanoscaled electrical devices. Especially carbon nanotubes are currently studied in great detail with respect to their electrical transport properties.^{1,2} It has been demonstrated that carbon nanotubes can behave like quantum wires exhibiting ballistic charge transports able to sustain very high current densities, exceeding 10^7 A/cm^2 .³ In addition, electric field-effect transistors from individual nanotubes have been reported.^{4,5} However, the reproducible implementation of nanotubes into electrical devices is complicated by the fact that the tubes exist in different chiralities and diameters.² Moreover, since the raw material consists of a dense network of closely connected nanotubes, individual tubes are often obtained by ultrasonic agitation, which might introduce defects into the tubes. Attempts to synthesize individual nanotubes directly on patterned surfaces have started only recently.⁶ Therefore, alternative types of nanowires that lack these drawbacks are of considerable interest. Inorganic materials like WS_2 nanotubes,^{7,8} silicon nanowires,⁹ or vanadium pentoxide nanotubes¹⁰ as well as molecules like DNA¹¹ become increasingly important in this respect. In the present study, we use vanadium pentoxide (V_2O_5) fibers as conducting wires with a thickness of molecular dimension. Individual V_2O_5 fibers, $\sim 1.5\text{ nm}$ in height and $\sim 10\text{ nm}$ in width, can be adsorbed in controllable density on chemically modified Si/SiO₂ surfaces.¹² Although pure V_2O_5 is a semiconductor with a band gap of $\sim 2.2\text{ eV}$,¹³ specific conductivities up to 1 S/cm have been reported for V_2O_5 xerogels.¹⁴ This behavior is attributed to hopping conduction between V^{5+} and V^{4+} impurity centers.¹⁵ In this letter, it will be shown that the electrical transport through unmodified V_2O_5 fibers

can be effectively modulated by the potential of a gate electrode, representing a new type of field-effect transistor (FET) based upon inorganic nanowires.

V_2O_5 fibers were synthesized from ammonium(meta)-vanadate and an acidic ion exchanger and deposited on chemically modified Si/SiO₂ substrates as reported recently.¹² The amount of V^{4+} impurity centers in V_2O_5 sols prepared by this method is found to be maximally 1%.¹⁶ Subsequently, 15 nm thick Au/Pd electrodes, separated by $\sim 100\text{ nm}$, were patterned on the fibers using electron beam lithography. A scanning force microscopy (SFM) image of the investigated sample is displayed in Fig. 1. The substrate was heavily doped by As^+ ion implantation and served as a back gate, which was separated from the electrodes by a thermally grown SiO₂ layer of thickness $d=300\text{ nm}$. At room temperature, the two-probe resistance of the V_2O_5 fibers ranged between 200 and 300 M Ω .

Figure 1 shows an SFM image of one of our samples. In this particular case, there are seven fibers between the middle two electrodes. The current-voltage characteristics obtained from this electrode pair are plotted in Fig. 2(a) at different temperatures for zero gate voltage ($V_G=0$). As temperature decreases, a nonohmic behavior is observed. Upon sweeping the gate voltage from -20 to $+20\text{ V}$ at $T=145\text{ K}$, the drain-source current (I_{DS}) increases as shown in Fig. 2(b). The conductance increase at positive gate voltage is attributed to the accumulation of electrons,¹⁷ and is in accordance with the known n -type semiconducting behavior of V_2O_5 .¹⁸ For higher temperatures, the conductance increases and the nonohmic behavior disappears with rather small gate dependence. The decrease of gate voltage dependence in the ohmic regime can be understood from the increase of relative ratio between the intrinsic carriers and the induced carriers by gate voltage, assuming generation of intrinsic carriers by thermal activation.

Up to the maximally applied electric field of 10^5 V/cm , no current saturation was observed, contrary to the conven-

^{a)}Electronic mail: gtkim@klizix.mpi-stuttgart.mpg.de

^{b)}Permanent address: Department of Physics and Condensed Matter Research Institute, Seoul National University, Seoul 151-742, Korea.

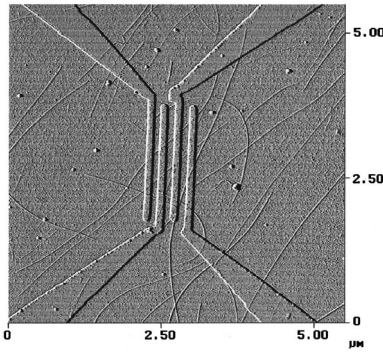


FIG. 1. SFM image of V_2O_5 fibers below Au/Pd electrodes, separated by ~ 100 nm. Current–voltage characteristics were measured between the middle two electrodes, which are connected by seven V_2O_5 fibers.

tional FET behavior.¹⁹ The charge distribution induced by the gate voltage as a function of the distance from the insulating layer is described by Eq. (1):²⁰

$$n = n_0 \left(1 + \frac{y}{\lambda_D \sqrt{2}} \right)^{-2}, \quad (1)$$

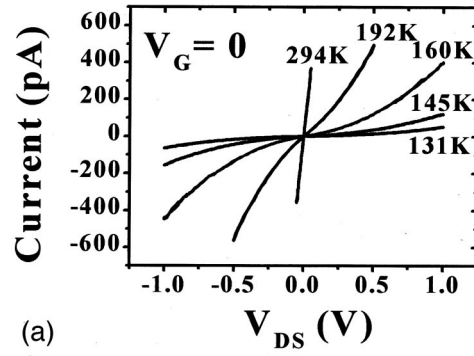
where y is the distance from the insulating layer and λ_D is Debye length given by the relation $\lambda_D = d_i (k_B T \sqrt{2}) / (q V_g)$, with d_i as thickness of the insulator and q the unit charge of electron. Using the values of $T = 145$ K, $d_i = 300$ nm, $V_g = 20$ V, the Debye length is estimated to 26.6 nm, which is considerably larger than the thickness of the individual V_2O_5 fibers (1.5 nm). As a consequence, a very high drain/source voltage would be required for pinch-off, which was not reached in our experiments.

The carrier mobilities are estimated from the linear regime of the I – V characteristic ($E < \sim 6 \times 10^3$ V/cm) following Eq. (2).²¹

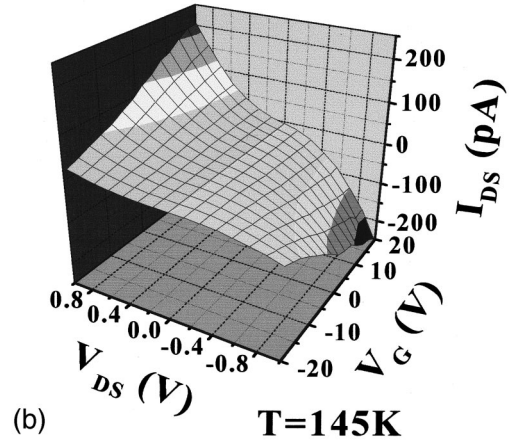
$$\frac{g_d}{\sqrt{g_m}} \sqrt{\frac{L V_d}{Z C_i}} = \sqrt{\mu} (V_g - V_0), \quad (2)$$

where g_d is the differential conductance $\partial I_{DS} / \partial V_{DS}$, g_m the transconductance $\partial I_{DS} / \partial V_G$, L the channel length (100 nm), Z the channel width (10 nm \times 7 fibers in our case), and C_i the capacitance of the SiO_2 layer per unit area which was taken as 1.2×10^{-12} F/cm².¹⁹ V_0 is the threshold voltage that accounts for the voltage drop of various origins across the insulator-semiconductor interface. In Fig. 3, the left term of Eq. (2) is plotted against gate voltage for $V_{DS} = 0.06$ V. Following Eq. (2), the slope gives the square root mobility at each gate voltage, and as the slope in this case is linear, the mobility is constant for gate voltage between -20 and $+20$ V. A mobility of 1.63×10^{-4} cm²/V s was obtained for $T = 145$ K, and the mobility increases with temperature as illustrated by the left inset of Fig. 3. From the slope of the left inset of Fig. 3, the activation energy is calculated to be $E_a = 0.18$ eV.²² In the right inset of Fig. 3, $-\sqrt{\mu} V_0$ vs $\sqrt{\mu}$ is plotted. From this slope, V_0 is estimated to be -16.7 V. Its negative sign confirms that the V_2O_5 fibers have n -type carriers (electrons).^{18,23}

Assuming that the nonohmic behavior at high drain/source voltages ($E > 10^4$ V/cm) is explained by small-polaron hopping,²⁴ the nonohmic regime can be fitted to Eq. (3):²⁴



(a)



(b)

FIG. 2. (a) Current–voltage characteristics obtained from the middle two electrodes (see Fig. 1) with zero gate voltage ($V_G = 0$ V) at different temperatures $T = 131, 145, 160, 192, 294$ K. (b) 3D plot of I/V curves in dependence of gate voltage at $T = 145$ K.

$$j = \frac{en\omega_{op}}{\pi} \sinh\left(\frac{eV_{DS}a}{2k_B T L}\right) \exp\left(-\frac{E_a}{k_B T}\right) = \alpha \sinh\left(\frac{eV_{DS}a}{2k_B T L}\right), \quad (3)$$

where ω_{op} is the optical phonon frequency, L the channel length, and a the nearest-neighbor hopping distance. Following this approach, we determined the best fitting parameters for each gate voltage and temperature. The fitting parameter except the sinh term in Eq. (3) was taken as α . Assuming the carrier concentration, n , is composed of the intrinsic carrier density, n_0 , and the induced carrier concentration, n_{ind} , n is

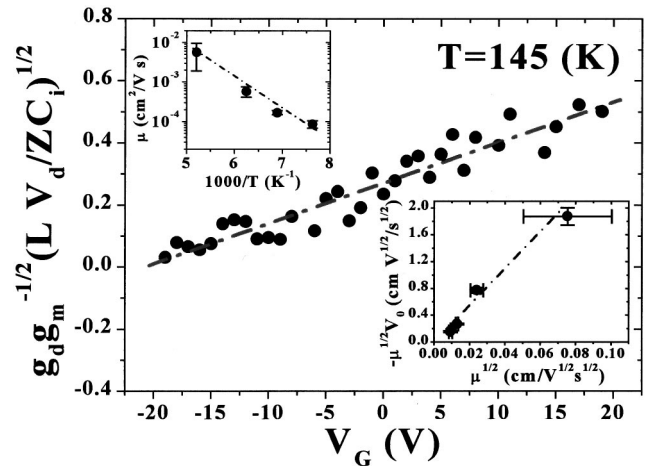


FIG. 3. Gate dependence of $(g_d / \sqrt{g_m}) (\sqrt{L V_d} / \sqrt{Z C_i})$ values at $T = 145$ K ($V_{DS} = 0.06$ V). Left inset: temperature dependence of mobilities. Right inset: relation between $-\sqrt{\mu} V_0$ and calculated square root of mobility.

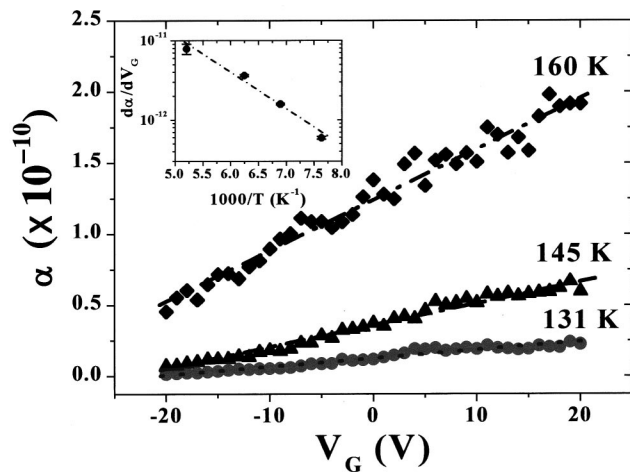


FIG. 4. Fitting parameter α depending on the gate voltage. Inset: plot of $\partial\alpha/\partial V_G$ against T^{-1} .

given by $n = n_0 + n_{\text{ind}} = n_0 + C_{\Sigma} V_g$, where C_{Σ} is the total capacitance between V_2O_5 fibers and gate electrode. Then, α can be expressed by Eq. (4):

$$\alpha = \frac{en_0\omega_{\text{op}}}{\pi} \exp\left(-\frac{E_a}{k_B T}\right) + \frac{eC_{\Sigma}\omega_{\text{op}}}{\pi} V_g \exp\left(-\frac{E_a}{k_B T}\right). \quad (4)$$

In Fig. 4, α was plotted against V_G , showing a linear dependence of gate voltage. In the inset of Fig. 4, $\partial\alpha/\partial V_G$ is plotted against $1000/T$. The slope of this curve corresponds to an activation energy of 0.092 eV. From the intercepts at $V_G = 0$, a slightly larger activation energy of $E_a = 0.114$ eV is obtained. Both values are smaller than the activation energy of $E_a = 0.17$ eV reported for thin bulk layers of V_2O_5 xerogels.²⁵ This difference may be understood from the fact that in our experiments, conduction proceeds along individual fibers, without interference from barriers represented by the interfiber contacts, as is the case for the entangled fibers in V_2O_5 xerogels. From the best fit of $ea/(2k_B TL) \sim 2$ (V^{-1}), the nearest-neighbor hopping distance is estimated to be ~ 4 nm, which is slightly less than half of the width of one individual V_2O_5 fiber. Taking into account the effect of contact resistance, the voltage drop along the fibers could be smaller than the applied voltage, and therefore this value for the nearest-neighbor hopping distance may be underestimated.

In summary, n -type enhancement FET-like behavior has been demonstrated for individual V_2O_5 fibers at low temperatures. The mobility was found to be almost independent of gate voltage and to be activated by temperature. Following the model of small polaron hopping conduction, the significant increase of conductivity at positive gate voltage was attributed to the increase of carrier concentration. At the present stage, the performance of nanofiber FET is limited due to the relatively high resistance of the vanadium pentox-

ide nanowires. The conductivity of the fibers might be increased by conversion into different vanadium oxides (like VO_2 or V_2O_3) or the formation of a conducting organic polymer layer²⁶ on top the fibers.

The authors are grateful to F. Schartner, U. Waizmann, and M. Riek for technical support. This work was supported by KISTEP under the Contract No. 98-I-01-04-A-026, Ministry of Science and Technology (MOST), Korea. Partial support for G.T.K. was received from the KOSEF research training fellowship program in Germany. M.B. is grateful to the Deutsche Forschungsgemeinschaft (DFG) for financial support.

- ¹J. Nygard, D. H. Cobden, M. Bockrath, P. L. McEuen, and P. E. Lindelof, *Appl. Phys. A: Mater. Sci. Process.* **69**, 297 (1999).
- ²R. Saito, G. Dresselhaus, and M. S. Dresselhaus, *Physical Properties of Carbon Nanotubes* (Imperial College Press, London, 1998).
- ³S. Frank, P. Poncharal, Z. L. Wang, and W. A. de Heer, *Science* **280**, 1744 (1998).
- ⁴S. J. Tans, M. H. Devoret, H. Dai, A. Thess, R. E. Smalley, L. J. Geerligs, and C. Dekker, *Nature (London)* **386**, 474 (1997).
- ⁵R. Martel, T. Schmidt, H. R. Shea, T. Hertel, and Ph. Avouris, *Appl. Phys. Lett.* **73**, 2447 (1998).
- ⁶H. T. Soh, C. F. Quate, A. F. Morpurgo, C. M. Marcus, J. Kong, and H. Dai, *Appl. Phys. Lett.* **75**, 627 (1999).
- ⁷A. Leist, S. Stauff, S. Loken, E. W. Finkh, S. Lütke, K. K. Unger, W. Assenmacher, W. Mader, and W. Tremel, *J. Mater. Chem.* **8**, 241 (1998).
- ⁸R. Tenne, L. Margulius, M. Genut, and G. Hodes, *Nature (London)* **360**, 444 (1992).
- ⁹A. M. Morales and C. M. Lieber, *Science* **279**, 208 (1998).
- ¹⁰M. E. Spahr, P. Bitterli, R. Nesper, M. Müller, F. Krumeich, and H. U. Nissen, *Angew. Chem. Int. Ed. Engl.* **37**, 1263 (1998).
- ¹¹H.-W. Fink and C. Schönenberger, *Nature (London)* **398**, 407 (1999).
- ¹²J. Muster, G. T. Kim, V. Krstic, J. G. Park, Y. W. Park, S. Roth, and M. Burghard, *Adv. Mater.* **12**, 420 (2000).
- ¹³P. A. Cox, *Transition Metal Oxides* (Clarendon Press, Oxford, 1992), Chap. 3.
- ¹⁴J. Bullot, O. Gallais, M. Gauthier, and J. Livage, *Appl. Phys. Lett.* **36**, 986 (1980).
- ¹⁵J. Livage, *Chem. Mater.* **3**, 526 (1991).
- ¹⁶N. Gharbi, C. Sanchez, J. Livage, J. Lemerle, L. Nejem, and J. Lefebvre, *Inorg. Chem.* **21**, 2758 (1982).
- ¹⁷C. Zhou, D. M. Newns, J. A. Misewich, and P. C. Pattnaik, *Appl. Phys. Lett.* **70**, 598 (1997).
- ¹⁸P. Kounavis, A. Vomvas, E. Mytilineou, M. Roilos, and L. Murawski, *J. Phys. C* **21**, 967 (1988).
- ¹⁹R. C. Haddon, A. S. Perel, R. C. Morris, T. T. M. Palstra, A. F. Hebard, and R. M. Fleming, *Appl. Phys. Lett.* **67**, 121 (1995).
- ²⁰G. Horowitz, R. Hajlaoui, R. Bourguiga, and M. Hajlaoui, *Synth. Met.* **101**, 401 (1999).
- ²¹G. Horowitz, R. Hailaoui, D. Fichou, and A. El Kassmi, *J. Appl. Phys.* **85**, 3202 (1999).
- ²²K. Honma, M. Yoshinaka, K. Hirota, O. Yamaguchi, J. Asai, and Y. Makiyama, *Mater. Res. Bull.* **31**, 531 (1996).
- ²³G. Horowitz, R. Hajlaoui, H. Bouchriha, R. Bourguiga, and M. Hajlaoui, *Adv. Mater.* **10**, 923 (1998).
- ²⁴H. Böttger and V. V. Bryksin, *Hopping Conduction in Solids* (VCH, Weinheim, 1985), p. 51.
- ²⁵See Table 2 in J. Bullot, P. Cordier, O. Gallais, M. Gauthier, and J. Livage, *J. Non-Cryst. Solids* **68**, 123 (1984).
- ²⁶C.-G. Wu, D. C. DeGroot, H. O. Marcy, J. L. Schindler, C. R. Kannewurf, Y.-J. Liu, W. Hirpo, and M. G. Kanatzidis, *Chem. Mater.* **8**, 1992 (1996).